ELSEVIER

Journal of Nuclear Materials 248 (1997) 299–305

journal of nuclear materials

Study of environmental effects on water-side corrosion of Zircaloy-2 fuel cladding

Y. Etoh [a], S. Shimada [a], M. Sasaki [b], T. Kogai [c], H. Hayashi [d], M. Kitamura [d], K. Tsuji [d,*,1], M. Yamawaki [e]

[a] *Nippon Nuclear Fuel Development Co., Ltd., 2163, Narita-cho, Oarai-machi, Higashi-Ibaraki-gun, Ibaraki-ken 311-13, Japan*
[b] *Hitachi Ltd., Hitachi Works, 1-1, Saiwai-cho, 3-chome, Hitachi-shi, Ibaraki-ken 317, Japan*
[c] *Toshiba Corp., Isogo Engineering Center, 8, Shinsugita-cho, Isogo-ku, Yokohama 235, Japan*
[d] *Nuclear Power Engineering Corporation, Fujita-Kanko-Toranomon Bldg., 6F, 17-1, 3-chome, Toranomon, Minato-ku, Tokyo 105, Japan*
[e] *University of Tokyo, 3-1, 7-chome, Hongo, Bunkyo-ku, Tokyo 113, Japan*

Abstract

A new BWR corrosion loop, with two identical rigs, has been designed and installed in the Halden reactor. In these rigs, β and γ emitters were placed to examine the effects of local radiation on cladding corrosion. Two types of cladding tubes, the 9 × 9 type made of corrosion-resistant Zircaloy-2 and the 8 × 8 RJ type made of nodular-sensitive Zircaloy-2, were irradiated under the same conditions in the two rigs for about one year. The tubes contained UO_2 and Al_2O_3 pellets. Visual inspections and oxide thickness measurements by eddy current were carried out to see the effects of β and γ emitters, heat flux, and different cladding tubes on corrosion behaviors. Nodular corrosion appeared on the 8 × 8 RJ tube, while a uniform oxide layer was observed on the 9 × 9 tube. Beta emitters enhanced the corrosion for both tubes, while γ emitters accelerated it only on the 8 × 8 RJ tube. The effect of heat flux was unclear from non-destructive inspections. © 1997 Elsevier Science B.V.

1. Introduction

Water-side corrosion of Zircaloy-2 fuel cladding tubes in a BWR is affected by a number of environmental factors, such as neutron flux, β and γ radiation, heat flux, and water chemistry. The main radiation effects regarding corrosion are the formation of radical species by radiolysis and radiation damage in both oxide film and metal. Fast neutron fluxes are known to change the microstructure and microchemistry of Zr alloys [1–4]. It was suggested from out-of-pile corrosion tests of irradiated materials that fast neutron irradiation improved nodular corrosion resistance of Zircaloy [5,6], while they accelerated the uniform corrosion rate [7]. There have been a few investigations on the radiation effects on oxide films. Electrical conductivity of stabilized ZrO_2 was measured under γ radiation [8] and electron irradiation [9]. Both studies showed increased electrical conductivity under radiation. Heat flux may affect the cladding corrosion behavior [10,11] through cladding temperature and boiling in the coolant water, which changes dissolved gas contents as well as impurity contents. The effects of water chemistry on cladding corrosion have been systematically investigated using a BWR simulated corrosion loop [11–13]. These tests showed that dissolved oxygen and nitrogen caused nodular corrosion and increased the oxide growth rate under the simulated BWR conditions. Some investigators have proposed that high energy β radiation accelerated corrosion due to water radiolysis [14,15].

In the present work, a new BWR simulated corrosion loop, with two identical rigs, has been designed and installed in the Halden reactor to investigate the separate effects of radiation and heat flux. To examine the effects of local radiation on cladding corrosion, β and γ emitters were placed in the flow tubes. Two fuel rods with corrosion-resistant and nodular-sensitive Zircaloy-2 cladding

* Corresponding author. Tel.: +81-29 266 2131; fax: +81-29 266 2589; e-mail: etoh@nfd.co.jp.

[1] Present affiliation: Chubu Electric Power Co., Inc.

PII S0022-3115(97)00127-X

Table 1
Target values of operating parameters

Coolant pressure	7.45 MPa
Saturation temperature	290°C
Flow rate	~ 2 m/s at rod bottom
Heat rate (UO_2 region)	
– 9×9 fuel rod	35 kW/m (axial average)
	30–35 kW/m (time average)
– 8×8 RJ fuel rod	38 kW/m (axial average)
	33–38 kW/m (time average)
Onset of boiling	~ 300 mm from rod bottom
Dissolved oxygen (inlet)	300 ± 50 ppb
Dissolved hydrogen (inlet)	20–40 ppb
Conductivity	0.1–0.3 μS/cm²
pH (room temperature)	6.5–7.5

Table 2
Dimensions of emitters and cladding tubes

Cladding type	β emitter		γ emitter		Cladding tube
	OD (mm)	ID (mm)	OD (mm)	ID (mm)	OD (mm)
8×8 RJ	19.2	18.36	20.45	18.36	12.27
9×9	17.03	16.23	18.6	16.23	11.18

tubes were irradiated under the same conditions, with both UO_2 and Al_2O_3 pellets to examine heat flux effect.

2. Experimental procedures

The BWR simulated corrosion loop system was designed to operate under typical BWR coolant chemistry (300 ppb O_2) and thermohydraulic parameters as shown in Table 1. Schematic representations of the BWR loop facility and the two rigs for the fuel rod irradiation are shown in Figs. 1 and 2, respectively. Each rig was inserted into a pressure flask capable of withstanding typical BWR pressure and temperature conditions. The flask was surrounded by booster rods which provide a fast neutron flux of

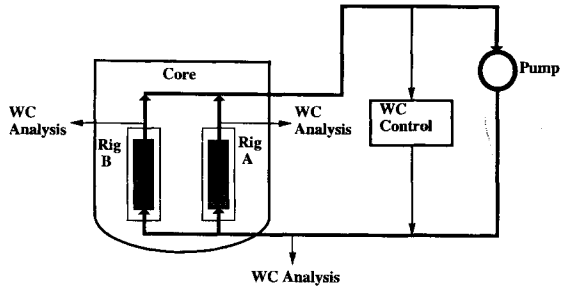

Fig. 1. Schematic of BWR simulated corrosion loop (WC: water chemistry).

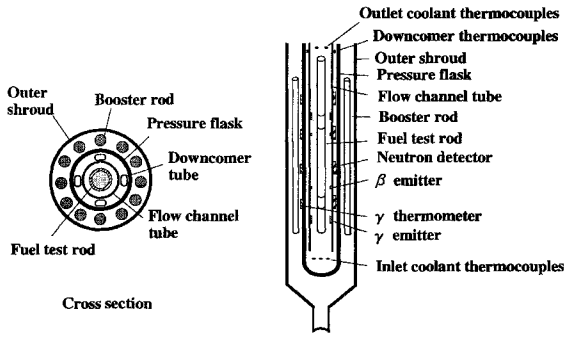

Fig. 2. Schematic of the two identical rigs.

5×10^{17} n/m²/s ($E > 1$ MeV) over a length of 800 mm. Platinum and hafnium sleeves were used as β and γ emitters, since both materials do not appreciably corrode or dissolve in water. The dimensions of emitters and cladding tubes are shown in Table 2. These emitters were placed at given heights on flow channel tubes. Both fuel rods were partly loaded with Al_2O_3 pellets to see the effect of heat flux on corrosion behavior. The configuration of the fuel rod and radiation emitters are shown in Fig. 3.

Two types of Zircaloy-2 cladding tubes were used to examine the effect of heat treatment of cladding tubes on corrosion behavior. One was nodular-sensitive, BWR 8 × 8 RJ type Zircaloy-2 cladding and the other was corrosion resistant, BWR 9 × 9 type Zircaloy-2. Corrosion resistant

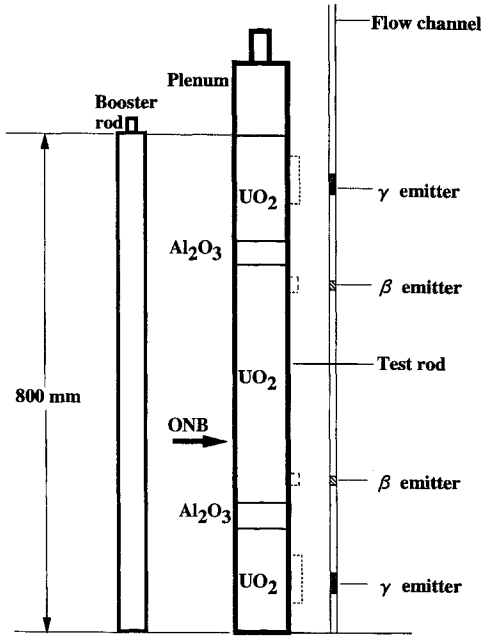

Fig. 3. Schematic of test rod and position of β and γ emitters.

Table 3
Test matrix

Thermohydraulic conditions		Standard conditions	Standard + β emitters	Standard + γ emitters
Boiling condition	heat flux	○	○	○
	non-heat flux	○	—	—
Non-boiling condition	heat flux	○	○	○
	non-heat flux	○	—	—

○: a test condition included in this program.
—: a test condition not included in this program.

Zircaloy-2 cladding was fabricated from a heat treated tubeshell, and the nodular-sensitive one, from a non-heat treated one.

The above test conditions covered the effects of boiling, heat flux, β and γ emitters, and heat treatment of the tubeshell. The test parameters are summarized in Table 3.

The irradiation test was continued for two cycles of the Halden reactor operation. After each cycle, the fuel cladding tubes were visually inspected and the oxide thickness was measured by an eddy current probe moved along the axial length of the rods at circumferential orientations 60° apart.

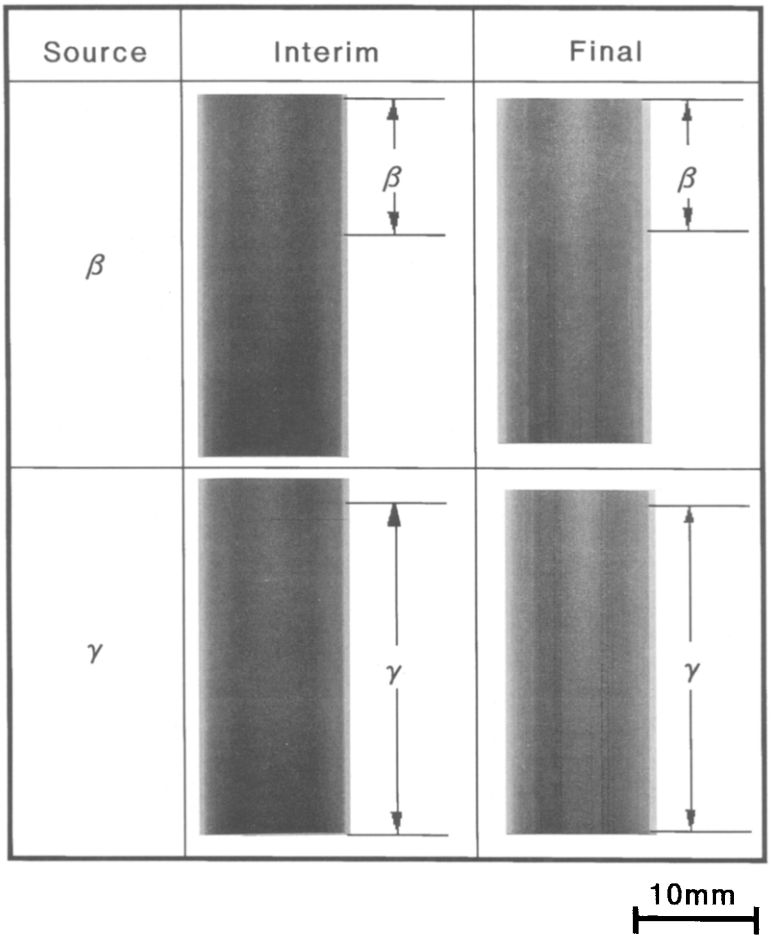

Fig. 4. Visual appearances of 8 × 8 RJ type cladding tube.

3. Results

3.1. Operating conditions

Data from the loop and rig instrumentation as well as the water chemistry monitors were logged at 15 min intervals. Collected data were coolant temperature, coolant flow rate, loop pressure, onset of boiling, steam quality, void fraction, fuel rod heat rating, booster rod heat rating, thermal neutron flux, γ flux, burnup of fuel rod, fast neutron fluence ($E > 1$ MeV), dissolved oxygen content, dissolved hydrogen content, and conductivity of coolant water. The main operating data are summarized in Table 4. The average thermal neutron fluxes at β and γ emitters were 1×10^{16} n/m^2/s, respectively. The coolant pressure, flow rate, linear heat rate, and temperature were almost the target values shown in Table 1. The fast neutron flux was a little smaller than the target. The boiling conditions were calculated by thermohydraulic data. The results indicated that bulk boiling started at about 400 to 600 mm from the bottom of fuel rod, which was a little higher than the target position (300 mm), and void fraction at the top was about 45%. Oxygen and hydrogen contents in coolant water ranged from about 200 to 400 ppb and 15 to 45 ppb, respectively. Although these data showed somewhat larger scattering than target values, the test rods were satisfactorily irradiated in this test.

3.2. Examination results

Non-destructive examinations of the test rods were carried out twice, as interim and final examinations. Interim examinations of the test rods were conducted after one irradiation cycle and final examinations were performed after two cycles. Typical results of visual inspections during interim and final examinations are shown in Figs. 4 and 5 for the 8×8 RJ and 9×9 type cladding tubes, respectively. Nodular corrosion appeared on the

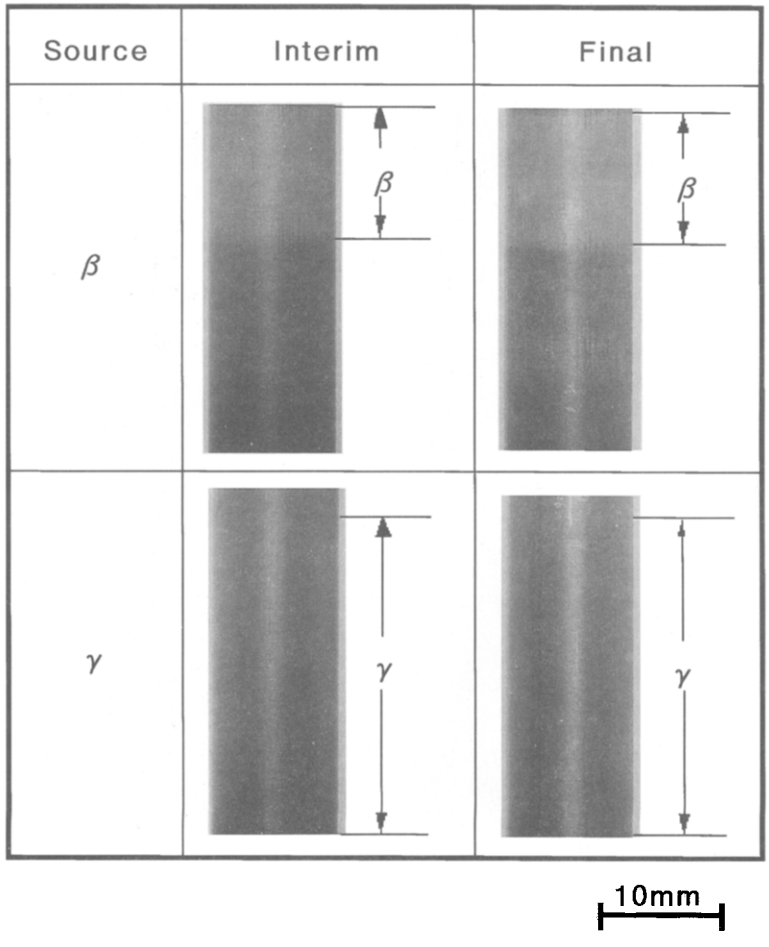

Fig. 5. Visual appearances of 9×9 type cladding tube.

Table 4
Operating data

Item	8 × 8 RJ cladding tube	9 × 9 cladding tube
Irradiation period (days)	183	
(EFPD)	177	
Burnup (GWd/t)	8.8	9.2
Linear heat rate (kW/m)	33–44	32–38
Neutron flux ($E > 1$ MeV; $\times 10^{17}$ n/m^2/s)	3.5–4.7	3.7–5.2
Neutron fluence ($E > 1$ MeV; $\times 10^{24}$ n/m^2)	6.2	7.2
Coolant pressure (MPa)	7.2–7.4	
Coolant flow rate (m/s)	1.5–2.5	1.8–2.8
Dissolved oxygen content (ppb, inlet)	200–400	
Dissolved hydrogen content (ppb, inlet)	15–45	

8 × 8 RJ type cladding tube and nodule density was higher on the surface facing the γ emitters than on the other regions and it was the highest on the surface facing the β emitters. No nodules were observed in the plenum region.

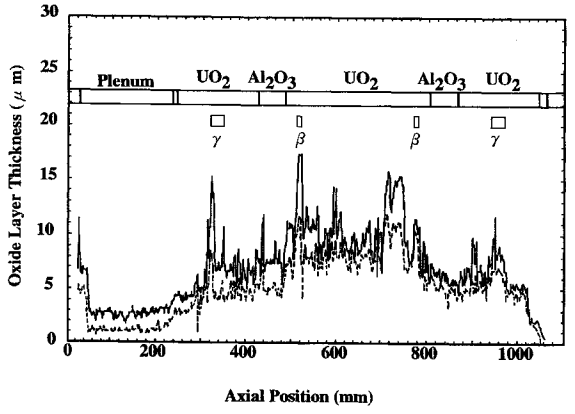

Fig. 6. Oxide layer thickness of 8×8 RJ type cladding tube (eddy current method). Solid line: final inspection, dotted line: interim inspection.

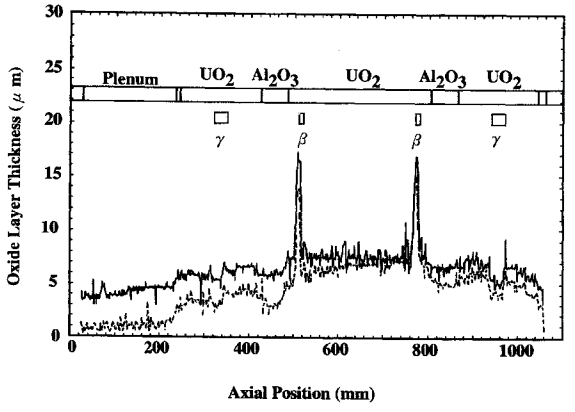

Fig. 7. Oxide layer thickness of 9×9 type cladding tube (eddy current method). Solid line: final inspection, dotted line: interim inspection.

There was no clear difference between UO_2 and Al_2O_3 pellet regions. The cladding surface was brown at the β emitter positions and boiling and heat flux positions, and black at the other positions. By contraries, the 9 × 9 type cladding tube showed no nodules and it was covered by a uniform oxide film only. This cladding tube was black along its whole length except for the areas facing the β emitters. These areas were covered with a whitish, uniform oxide layer. The effects of γ emitters, heat flux, and boiling were unclear from the visual inspection.

The oxide thickness was measured along the axial direction of the fuel rods by the eddy current method at the times of interim and final examinations. Examples of typical thickness profiles are shown in Figs. 6 and 7 for 8 × 8 RJ and 9 × 9 type cladding tubes, respectively. Both figures include the interim and final measurement profiles. These profiles indicated that, in general, the oxide layer grew rapidly during the first cycle and the oxide thickness tended to saturate during the second cycle. The β emitter positions showed drastic acceleration of corrosion on both 8 × 8 RJ and 9 × 9 type cladding tubes. This effect was more distinct for the 9 × 9 than for the 8 × 8 RJ type cladding tubes due to the former having a thinner oxide on the other areas. The γ emitter positions showed accelerated corrosion on only 8 × 8 RJ type cladding tube and no distinct effect on 9 × 9 type. Regarding heat flux, it was difficult to see the effect on corrosion from the eddy current profiles for both claddings.

Thus, the results of visual inspection coincided well with those of eddy current measurements. Based on these results, β emitters enhanced the corrosion of both types of cladding tubes, but γ emitters affected corrosion of the 8 × 8 RJ type only, and heat flux did not show any clear effects for both types of cladding tubes.

4. Discussion

A difference in corrosion behavior was observed between the two types of cladding tubes. The 8 × 8 RJ type

Zircaloy-2 cladding tube was sensitive to nodular corrosion in this experiment, while the 9×9 type Zircaloy-2 cladding tube had high nodular corrosion resistance. Nodular corrosion resistant Zircaloy-2 cladding tube was produced from heat treated tubeshell. This heat treatment is an $\alpha + \beta$ quench from the outer surface and it affects the size distribution of the second phase particles in Zircaloy-2. Nodular corrosion resistant, 9×9 type Zircaloy-2 had smaller size particles than nodular corrosion sensitive, 8×8 RJ type Zircaloy-2. TEM measurements of the particle gave 85 nm for the 9×9 type Zircaloy-2 and 207 nm for the 8×8 RJ type Zircaloy-2.

Zircaloy-2 consists of Zr, Sn, Fe, Cr, and Ni. The last three elements were added to improve corrosion resistance but their solution limits are very small in the α-Zr or Zr–Sn matrix [16]. Most of the added Fe, Cr, and Ni exist in the second phase particles. Nodular corrosion resistance was improved by increasing dissolved Fe, Cr, and Ni contents [5,6]. Second phase particles, consisting of Zr–Fe–Cr and Zr–Fe–Ni, dissolved during irradiation under BWR conditions [1–4]. Therefore, a smaller particle size leads to faster dissolution of these elements and improves nodular corrosion resistance during irradiation. This is one possible explanation for the effect of tubeshell heat treatment on nodular corrosion resistance of Zircaloy-2.

The acceleration of corrosion by β emitters was clearly observed for both types of cladding tubes. The acceleration effect of γ emitters was confirmed for only the 8×8 RJ type. These radiation effects might be due to formation of a high concentration of radicals near the surface of the oxide film by radiolysis of water [14,15] and/or an increase of electric conductivity in the oxide film [8,9]. For normal BWR conditions, coolant water includes dissolved oxygen of several hundred ppb, so that oxidizing radical species would be formed under irradiation. Therefore, a severer oxidizing environment would be produced near the β and γ emitters, and corrosion would be accelerated. Measured electric conductivity of stabilized ZrO_2 [8,9] was considered to be induced by ionic diffusion. It might be considered that radiation accelerated the diffusion of O^{2-} and enhanced the oxidation rate. These two mechanisms and their synergistic effect are possible explanations for the effect of β and γ emitters on corrosion of Zircaloy-2.

The heat flux effect was expected [10,11] but no clear difference between UO_2 and Al_2O_3 pellet positions was observed from both visual inspections and oxide thickness measurements by the eddy current method. From the eddy current profile, a little bit thinner oxide thickness was observed at the Al_2O_3 pellet positions of the 9×9 type cladding tube. But it is difficult to confirm that this difference is due to the heat flux effect. For the 8×8 RJ type cladding tube, scattering of thickness data was larger than for the 9×9 type due to the formation of nodular corrosion and the heat flux effect could not be observed. This result indicated that the heat flux effect was too small to detect by the eddy current method.

5. Conclusions

A new BWR simulated corrosion loop has been designed, installed and operated in the Halden reactor and the effects of β and γ emitters, heat flux and heat treatment of cladding tubes on corrosion were investigated. The irradiation test gave the following results.

(1) Nodular corrosion appeared only on the 8×8 RJ type cladding tube. A uniform oxide layer was observed on the 9×9 type cladding tube.

(2) Both types of cladding tubes showed the acceleration of corrosion on the surface facing the β emitters.

(3) Only 8×8 RJ type cladding tube showed acceleration of corrosion on the surface facing the γ emitters.

(4) The effect of heat flux on corrosion behavior was not clarified by non-destructive examinations.

Acknowledgements

This study is a part of the phase-1 program, 'Demonstration Test on BWR 9×9 Fuel in Japan'. The program aims at evaluating corrosion performance of corrosion-resistant Zircaloy-2 at high burnup regions and is under the sponsorship of the Ministry of International Trade and Industry (MITI). The authors acknowledge MITI for its support.

References

[1] W.J.S. Yang, R.P. Tucker, B. Cheng, R.B. Adamson, J. Nucl. Mater. 138 (1986) 185.
[2] M. Griffiths, R.W. Gilbert, G.J.C. Carpenter, J. Nucl. Mater. 150 (1987) 53.
[3] Y. Etoh, S. Shimada, J. Nucl. Sci. Technol. 29 (1992) 358.
[4] Y. Etoh, S. Shimada, J. Nucl. Mater. 200 (1993) 59.
[5] Y. Etoh, K. Kikuchi, T. Yasuda, S. Koizumi, M. Oishi, Proc. Int. Topical Meeting on LWR Fuel Performance, Avignon, 1991, p. 691.
[6] Y. Etoh, S. Shimada, K. Kikuchi, K. Kawai, J. Nucl. Sci. Technol. 29 (1992) 1173.
[7] B. Cheng, R.M. Kruger, R.B. Adamson, ASTM STP 1245 (1994) 400.
[8] T-K. Kang, I-H. Kuk, Y. Katano, N. Igawa, H. Ohno, J. Nucl. Mater. 209 (1994) 321.
[9] K. Shiiyama, C. Kinoshita, H. Suzuki, T. Izu, M. Kutsuwada, S. Matsumura, Nucl. Instrum. Methods B91 (1994) 284.
[10] Y. Etoh, J. Nucl. Sci. Technol. 26 (1989) 752.
[11] K. Ito, S. Shimada, H.A. Levin, R.B. Adamson, J.-S.F. Chen, M. Oguma, B. Cheng, T. Ikeda, K. Takei, Y. Ishii, Proc. Int. Topical Meeting on LWR Fuel Performance, West Palm Beach, FL, 1994, p. 273.
[12] S. Shimada, C.C. Lin, B. Cheng, T. Ikeda, M. Oguma, K. Takei, Parametric Tests of the Effect of Water Chemistry Impurities on Corrosion of Zr-Alloys under Simulated BWR Condition, IAEA Technical Committee Meeting on Influence of Water Chemistry on Fuel Cladding Behavior, 1993.

[13] M. Aomi, T. Kogai, S. Shimada, N. Ichikawa, E. Ibe, Y. Ishii, B. Cheng, D. Lutz, Evaluation of Zircaloy Corrosion under Various Water Chemistries in a BWR Simulation Loop, Proc. Int. Conf. on Water Chemistry of Nuclear Reactor Systems, Bournemouth, UK, 1996.
[14] C. Lemaignan, J. Nucl. Mater. 187 (1992) 122.
[15] J.-S.F. Chen, R.B. Adamson, Proc. Int. Topical Meeting on LWR Fuel Performance, West Palm Beach, FL, 1994, p. 309.
[16] D. Charquet, R. Harn, E. Ortlieb, J.P. Gros, J.F. Wadier, ASTM STP 1023 (1989) 405.